Asymmetric functional contributions of acidic and aromatic side chains in sodium channel voltage-sensor domains

Stephan A. Pless,[1,2] Fisal D. Elstone,[1] Ana P. Niciforovic,[1] Jason D. Galpin,[1,3] Runying Yang,[1] Harley T. Kurata,[1] and Christopher A. Ahern[1,2,3]

[1]Department of Anesthesiology, Pharmacology and Therapeutics, and [2]Department of Cellular and Physiological Sciences, University of British Columbia, Vancouver, British Columbia V6T 1Z3, Canada

[3]Department of Molecular Physiology and Biophysics, University of Iowa, Iowa City, IA 52242

Voltage-gated sodium (Na_V) channels mediate electrical excitability in animals. Despite strong sequence conservation among the voltage-sensor domains (VSDs) of closely related voltage-gated potassium (K_V) and Na_V channels, the functional contributions of individual side chains in Na_v VSDs remain largely enigmatic. To this end, natural and unnatural side chain substitutions were made in the S2 hydrophobic core (HC), the extracellular negative charge cluster (ENC), and the intracellular negative charge cluster (INC) of the four VSDs of the skeletal muscle sodium channel isoform ($Na_V1.4$). The results show that the highly conserved aromatic side chain constituting the S2 HC makes distinct functional contributions in each of the four Na_V domains. No obvious cation–pi interaction exists with nearby S4 charges in any domain, and natural and unnatural mutations at these aromatic sites produce functional phenotypes that are different from those observed previously in K_v VSDs. In contrast, and similar to results obtained with K_v channels, individually neutralizing acidic side chains with synthetic derivatives and with natural amino acid substitutions in the INC had little or no effect on the voltage dependence of activation in any of the four domains. Interestingly, countercharge was found to play an important functional role in the ENC of DI and DII, but not DIII and DIV. These results suggest that electrostatic interactions with S4 gating charges are unlikely in the INC and only relevant in the ENC of DI and DII. Collectively, our data highlight domain-specific functional contributions of highly conserved side chains in Na_V VSDs.

INTRODUCTION

Voltage-gated sodium (Na_v) channels regulate the rapid flux of sodium ions across cell membranes and are thus important for the generation of both cardiac and neuronal action potentials (Hille, 2001; Catterall, 2010). Mammalian Na_v channels consist of four domains (DI–DIV) that are connected by cytoplasmic linkers of varying length. Each domain consists of six α-helical transmembrane segments (S1–S6), with S1–S4 making up the voltage-sensor domain (VSD) and S5–S6 constituting the pore domain. In response to a depolarizing voltage pulse, the S4 helices in the VSDs undergo an upward movement, which triggers a conformational change that leads to opening of the pore domain. In Na_v channels, this opening transition is followed by a rapid decrease in sodium conductance as a result of channel inactivation, a process that is thought to be mediated by a "hinged-lid" mechanism involving a highly conserved region in the DIII–DIV linker (West et al., 1992).

Recently published high resolution structures of homotetrameric bacterial Na_v channels demonstrated that many structural features of the voltage-gated potassium (K_v) channel family appear to be conserved in bacterial Na_v channels (Payandeh et al., 2011, 2012; McCusker et al., 2012; Zhang et al., 2012). Although the VSDs of K_v channels have gained much experimental attention, far less is known about the molecular function of VSDs in Na_v channels. This is of particular interest because of the proposed nonequivalent functional contributions of each Na_v channel domain to gating (Yang and Horn, 1995; Cha et al., 1999; Sheets et al., 1999; Chanda and Bezanilla, 2002; Bosmans et al., 2008; Capes et al., 2012; Goldschen-Ohm et al., 2013). The basis for domain-specific contributions is unknown, but one possibility is that highly conserved residues make distinct functional contributions because of subtle differences in the local domain architecture.

In this study, we focus on three regions in the rat skeletal sodium channel isoform ($Na_v1.4$) VSDs considered to be critical for the function of voltage-gated ion channels: the S2 hydrophobic core (HC), comprising a highly

Correspondence to Christopher A. Ahern: christopher-ahern@uiowa.edu

S.A. Pless's present address is Center for Biopharmaceuticals, Dept. of Drug Design and Pharmacology, University of Copenhagen, 2100 Copenhagen, Denmark.

Abbreviations used in this paper: ENC, extracellular negative charge cluster; ESP, electrostatic surface potential; HC, hydrophobic core; INC, intracellular negative charge cluster; K_v, voltage-gated potassium; Na_v, voltage-gated sodium; SSI, steady-state inactivation; UAA, unnatural amino acid; VSD, voltage-sensor domain.

The Rockefeller University Press $30.00
J. Gen. Physiol. Vol. 143 No. 5 645–656
www.jgp.org/cgi/doi/10.1085/jgp.201311036

conserved aromatic side chain in S2, as well as the extracellular negative charge cluster (ENC) and the intracellular negative charge cluster (INC), which contain conserved acidic side chains in S1, S2, and S3 (Fig. 1). The S2 HC is an aromatic side chain in virtually all voltage-gated ion channels and has recently been studied extensively with computational, functional, and structural methods in K_v channels (Tao et al., 2010; Delemotte et al., 2011; Lacroix and Bezanilla, 2011; Lin et al., 2011; Pless et al., 2011b; Schwaiger et al., 2011, 2013; Cheng et al., 2013). In contrast, the equivalent side chain in Na_v channels has not been studied, despite the fact that the equivalent aromatic side chains (tyrosine [Tyr] in DI, phenylalanine [Phe] in DII–DIV) are absolutely conserved among Na_v channels. Similarly, the acidic side chains that constitute the ENC and INC of voltage-gated ion channels contribute three to four highly conserved negative charges (Fig. 1) and have been examined in detail in K_v channels (Papazian et al., 1995; Planells-Cases et al., 1995; Seoh et al., 1996; Tiwari-Woodruff et al., 1997; Sato et al., 2002, 2003; Zhang et al., 2007; Pless et al., 2011b). However, their functional contributions remain largely unknown in Na_v channels, although several recent studies have implicated these side chains in channel function (DeCaen et al., 2008, 2009, 2011; Paldi and Gurevitz, 2010; Lin et al., 2011; Yarov-Yarovoy et al., 2012; Groome and Winston, 2013).

Here, we used conventional mutagenesis along with the in vivo nonsense suppression method for the incorporation of unnatural amino acids (UAAs) (Nowak et al., 1998; Pless and Ahern, 2013) to gain a better understanding of the functional contributions of highly conserved side chains in the HC, ENC, and INC of the four VSDs of a mammalian Na_v channel. In particular, we set out to decipher potential similarities and differences between the VSDs of K_v and Na_v channels, as well as putative functional diversity among individual Na_v domains.

MATERIALS AND METHODS

Molecular biology and in vivo nonsense suppression

Positions 151, 161, 168, 171, 197, 598, 621, 624, 646, 1051, 1069, 1076, 1079, 1373, 1396, 1399, or 1420 of $rNa_v1.4$ (in pBASTA) were mutated by conventional site-directed mutagenesis to code for leucine (Leu), asparagine (Asn), aspartic acid (Asp), Gln, Glu, or a TAG (amber) stop codon (see Results for details). mRNA was transcribed using a mMessage mMachine T7 kit (Ambion) after linearization with NotI. Stage V–VI oocytes were harvested from *Xenopus laevis* frogs, injected, and incubated as described previously (Pless et al., 2011a). Recordings were performed 12–24 h after injection. Phe and trifluoro-Phe (3,4,5-F_3-Phe or F_3-Phe) were purchased from AsisChem, Inc., and Sigma-Aldrich. Nitrohomoalanine (Nha) and 2-amino-3-indol-1-yl-propionic acid (Ind) were synthesized as described previously (Pless et al., 2011b; Lacroix et al., 2012). The in vivo nonsense suppression method was performed as detailed previously (Nowak et al., 1998). In brief, UAAs were nitroveratryloxycarbonyl (NVOC) protected and activated as the cyanomethyl ester for subsequent coupling to the dinucleotide pdCpA (Thermo Fisher Scientific). The resulting aminoacyl dinucleotide was ligated to an in vitro–generated modified tRNA from *Tetrahymena thermophila*. NVOC deprotection of the aminoacylated tRNA-aa was achieved through UV irradiation directly before coinjection with channel mRNA into *Xenopus* oocytes. In a typical experiment, 10–80 ng of tRNA-aa, 25–50 ng of channel mRNA, and 5–10 ng of β1 subunit mRNA were injected in a total volume of 50 nl. To test for nonspecific incorporation of endogenous amino acids and/or recharging of the injected tRNA, sodium channel mRNAs containing individual TAG stop codons in positions 161, 168, 171, 598, 621, 624, 1076, 1079, 1373, 1396, or 1399 were coinjected with Nha-acylated tRNA or tRNA ligated to pdCpA but not coupled to a UAA. However, in positions 197, 598, 624, 646, 1069, 1079, 1101, 1373, and 1420, we observed (a) very small or no currents with acylated tRNA, or (b) significant currents in the absence of an acylated tRNA (pdCpA-tRNA only) or currents that were not significantly different from those elicited by injection of acylated tRNA (see Fig. S1 for details). Consequently, only positions 161, 168, 171, 621, 1076, 1396, and 1399 were used for incorporation of UAAs. Note that because of the temporary unavailability of pdCpA during the revision process of this paper, Nha could not be introduced in position 1051 using the approach described above (see Fig. 2).

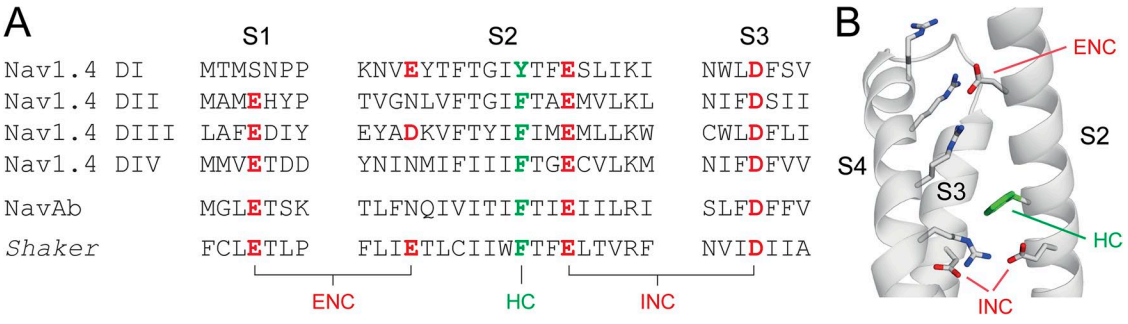

Figure 1. Highly conserved acidic and aromatic side chains in the VSDs of voltage-gated ion channels. (A) Sequence alignment of S1, S2, and S3 segments of different voltage-gated ion channels: $Na_v1.4$, NavAb, and *Shaker* potassium channels. The S2 HC is highlighted in green; negatively charged side chains in the ENC and the INC are highlighted in red. (B) Structure of the Na_vAb VSD (Protein Data Bank accession no. 3RVY; Payandeh et al., 2011). The conserved S4 arginines, as well as conserved acidic and aromatic side chains in S2 and S3, are shown in stick representation (note that S1 was omitted for clarity).

Electrophysiology

Voltage-clamped sodium currents were recorded with two-electrode voltage clamp using two glass microelectrodes with resistances between 0.1 and 1 MΩ (backfilled with 3 M KCl). Recordings were performed at 20–22°C in a standard Ringer's solution (mM): 116 NaCl, 2 KCl, 1 $MgCl_2$, 0.5 $CaCl_2$, and 5 HEPES, pH 7.4; the recording chamber was perfused through an automated perfusion system (Valve Bank 8; AutoMate Scientific). A voltage clamp (OC-725C; Warner Instruments) was used; the holding potential was −100 mV in all experiments. All data were mean ± SEM.

Online supplemental material

Fig. S1 compares the currents recorded from Nav1.4-TAG mRNA after coinjection with either Nha-pdCpA-tRNA or pdCpA-tRNA (lacking a conjugated amino acid). The online supplemental material is available at http://www.jgp.org/cgi/content/full/jgp.201311036/DC1.

RESULTS

Charge plays a critical role at the ENC positions in DI and DII only

We sought to determine the potential functional contribution of negative charge to channel function in the ENC and INC by individually neutralizing the acidic side chains occupying these positions. Given that the side chains reside in an area likely critical for channel function, we sought to use subtle analogues of naturally occurring amino acids. In particular, we attempted to incorporate the UAA Nha, an isosteric but neutral analogue of Glu, in which the terminal (δ) carbon that forms the carboxylate functional group is replaced by a nitrogen. Nha offers a significant advantage over replacing Glu by the most subtle naturally occurring side chain, Gln: although neutral, Gln can act as a potent hydrogen bond donor, which can cause significant (but nonspecific) perturbations in channel function (Cashin et al., 2007; Pless et al., 2011b,c). Importantly, Nha, like Glu, does not have any propensity to act as a hydrogen bond donor and is thus an ideal neutral replacement for Glu. In contrast, the nitro analog of Asp is chemically not compatible with the in vivo nonsense suppression approach (Cashin et al., 2007), and we thus replaced Asp residues with Asn side chains via conventional site-directed mutagenesis (see below).

First, we focused on the acidic ENC side chain in S2 (Fig. 1), which is a negatively charged side chain in most K_v channels, as well as in DI and DIII of Na_v channels. In particular, we sought to determine possible contributions of charge to channel function by individually neutralizing these side chains in DI and DIII and by introducing an acidic side chain in DII. As shown in Fig. 2 A, we were able to successfully incorporate Nha in position 161 in the DI S2 ENC. The resulting mutant (Glu-161TAG + Nha) showed a drastic (>10-mV) right-shift in the $V_{1/2}$ for activation with no change in the slope factor, likely indicating a significant destabilization of the channel open state as a consequence of side chain neutralization (Fig. 2 B and Table 1). In DII S2, the ENC is occupied by a neutral side chain, Asn. Recently, it was demonstrated that introducing a basic side chain (lysine [Lys]) in the equivalent position in $hNa_v1.4$ results in a right-shifted G-V (Groome and Winston, 2013), a finding consistent with the notion of charge at this position potentially being critical for open-state stability (see above and Pless et al., 2011b). We thus reasoned

TABLE 1

Electrophysiological effects of neutralizing side chains in the ENC and INC

Construct	Location	G-V		SSI		*n*
		$V_{1/2}$	dx	$V_{1/2}$	dx	
WT	n/a	−26.3 ± 0.5	3.0 ± 0.1	−52.9 ± 0.5	5.7 ± 0.1	17
Ser151Glu	DI S1 (ENC)	−32.7 ± 1.1[a]	2.5 ± 0.2	−53.2 ± 0.9	5.4 ± 0.1	6
Glu598Gln	DII S1 (ENC)	−17.4 ± 0.7[a]	2.7 ± 0.2	−50.6 ± 0.8	6.7 ± 0.4	5
Glu1051Gln	DIII S1 (ENC)	−24.8 ± 0.7	2.5 ± 0.2	−46.1 ± 0.9[a]	5.0 ± 0.2[a]	6
Glu1373Gln	DIV S1 (ENC)	−27.3 ± 2.6	3.3 ± 0.2	−40.7 ± 1.2[a]	4.6 ± 0.1[a]	6
Glu161TAG + Nha	DI S2 (ENC)	−14.8 ± 0.3[a]	3.1 ± 0.1	−50.0 ± 0.2[a]	5.9 ± 0.1	3
Asn614Asp	DII S2 (ENC)	−32.0 ± 0.6[a]	3.2 ± 0.1	−57.2 ± 1.0[a]	5.4 ± 0.3	5
Asp1069Asn	DIII S2 (ENC)	−27.3 ± 0.7	2.7 ± 0.2	−50.7 ± 0.5	5.2 ± 0.2	5
Glu171TAG + Nha	DI S2 (INC)	−26.8 ± 0.7	3.0 ± 0.1	−52.9 ± 0.9	5.1 ± 0.2[a]	9
Glu624Gln	DII S2 (INC)	−22.7 ± 0.5[a]	3.6 ± 0.1	−51.6 ± 0.8	6.0 ± 0.8	6
Glu1079Gln	DIII S2 (INC)	−27.6 ± 1.0	3.0 ± 0.2	−55.6 ± 1.0	5.4 ± 0.2	6
Glu1399TAG + Nha	DIV S2 (INC)	−24.7 ± 0.5	3.2 ± 0.1	−46.2 ± 0.8[a]	7.1 ± 0.2[a]	6
Asp197Asn	DI S3 (INC)	−26.0 ± 0.6	3.4 ± 0.2	−52.9 ± 0.8	7.1 ± 0.4[a]	7
Asp646Asn	DII S3 (INC)	−22.5 ± 1.6	2.9 ± 0.2	−55.7 ± 1.6	6.0 ± 0.8	9
Asp1101Asn	DIII S3 (INC)	−27.6 ± 0.7	3.3 ± 0.1	−58.1 ± 0.7[a]	6.5 ± 0.4	7
Asp1420Asn	DIV S3 (INC)	−25.8 ± 1.4	3.3 ± 0.2	−46.2 ± 1.7[a]	6.9 ± 0.3[a]	7

Displayed are the values for the midpoints ($V_{1/2}$) and the slope factors (dx) of the G-V relations and the SSI, as well as the number of experiments conducted (*n*).

[a]Statistical difference to WT values in an unpaired *t* test ($P < 0.01$).

that if charge played a major role for open-state stability, introducing an acidic side chain in position 614 should increase open-state stability. Indeed, the Asn614Asp mutant showed a 6-mV left-shift in the G-V with no effect on the slope (Fig. 2 B and Table 1). Although we were unable to introduce Nha in the DIII S2 ENC (position 1069; see Materials and methods for details), even the neutralization using conventional side chain replacement (Asp1069Asn) did not affect the G-V (Fig. 2 B and Table 1). Reminiscent of DII, the DIV S2 ENC position is occupied by a neutral side chain, Asn1389. However, this side chain had recently been mutated to both basic and acidic side chains without affecting channel activation in $hNa_v1.4$ (Groome and Winston, 2013) and was thus not further studied here. Similar to the effects observed on the G-V relations, entry into fast inactivation and steady-state inactivation (SSI) was affected only by mutations in DI and DII (Glu161TAG + Nha and Asn614Asp), but not in DIII (Fig. 2 C and Table 1).

Further, we sought to investigate the functional role of charge in the S1 ENC (Fig. 1). Replacing the neutral Ser side chain with Glu resulted in a significant left-shift of the G-V, whereas neutralization of the equivalent side chain in DII (Glu598Gln) resulted in a right-shifted G-V (Fig. 2, A and B, and Table 1). In contrast, replacing the negatively charged side chains in DIII and DIV had no effect on the G-V relations (Fig. 2, A and B, and Table 1), a finding consistent with similar experiments performed on $hNa_v1.4$ (Groome and Winston, 2013). Importantly, both the neutralization in DIII (Glu1051Gln) and DIV (Glu1373Gln) shifted the SSI parameters significantly toward more depolarized potentials, whereas entry into fast inactivation was slower for neutralization in DII (Glu598Gln) and DIV (Glu1373Gln) only (Fig. 2 F and Table 1).

Charge plays a minor role in the INC positions of all four domains

The INC consists of two highly conserved acidic side chains near the intracellular end of S2 and S3, respectively (Fig. 1). To investigate the functional basis for the very high degree of conservation of these acidic side chains we successfully introduced Nha in DI and DIV (Glu171TAG + Nha and Glu1399TAG + Nha, respectively)

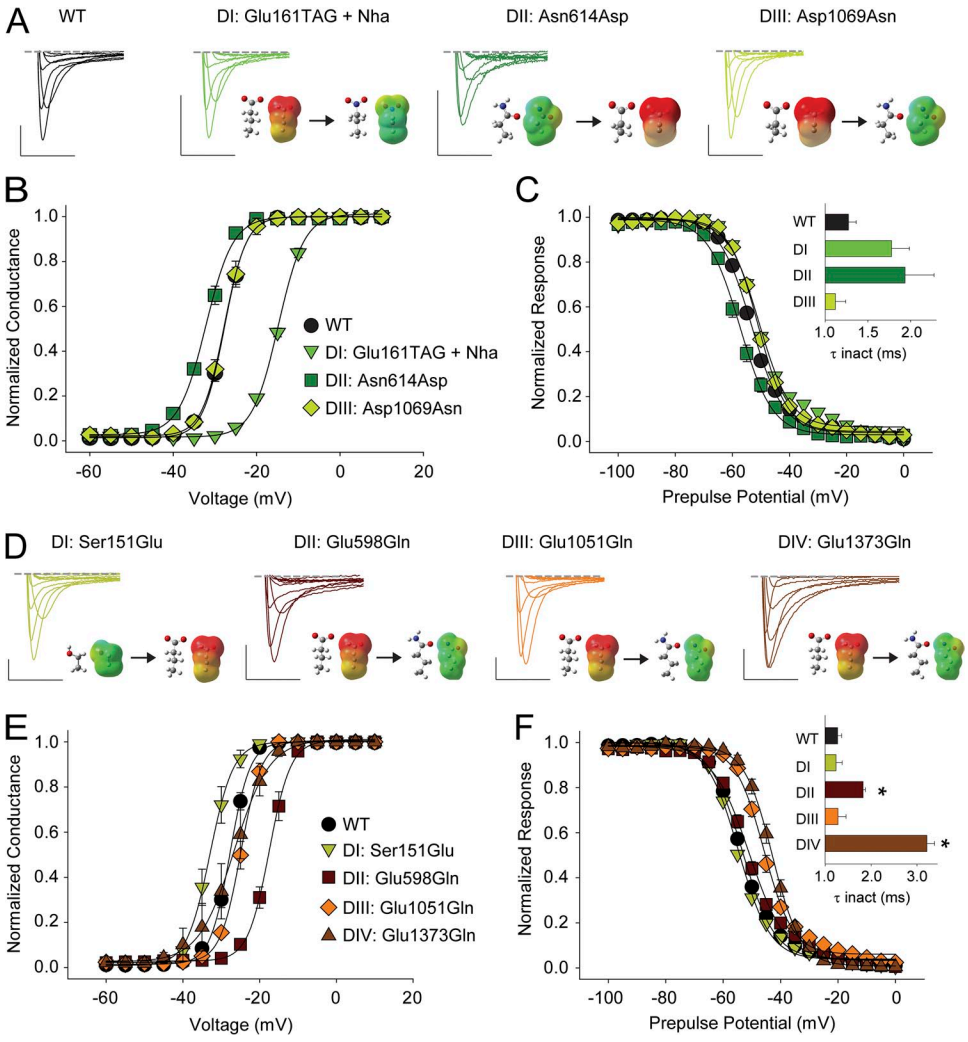

Figure 2. ENC electrostatic contributions are critical in DI and DII only. (A and D) Sample traces for currents recorded for WT and mutants at the S1 and the S2 ENC in DI–DIV. (B, C, E, and F) G-V (B and E) and SSI curves (C and F) for WT and mutants at the S1 and the S2 ENC; the insets in C and F show a bar graph representing the average time constants for fast inactivation (τ) for a depolarizing voltage step to −15 mV for WT and the mutants; *, statistical difference to WT values in an unpaired *t* test ($P < 0.01$). Note that Asn1389 in the S2 ENC in DIV had been mutated to both acidic and basic side chains previously with no functional consequence and was thus not studied further here (Groome and Winston, 2013). Bars: horizontal, 5 ms; vertical, 200 nA. Voltage steps were from −40 to +20 mV in 10-mV increments. Insets show energy-minimized structures and ESP maps of side chains (red, −100 kcal/mol; green, 0 kcal/mol; blue, +100 kcal/mol; see Pless et al., 2011b, for details).

and, importantly, observed no changes in the G-V relations (Fig. 3 A). Attempts to introduce Nha in equivalent positions in DII and DIII were unsuccessful (see Materials and methods for details); however, the conventional Gln mutation was well tolerated and produced channels with a normal G-V in DIII (Glu1079Gln), and only had a small effect in DII (Glu624Gln) (Fig. 3 A and Table 1). Although the entry into fast inactivation was slowed by neutralizations in both DII and DIV, the voltage dependence of SSI was only changed in DIV (Fig. 3 B).

Next, we sought to determine if the highly conserved negative charge in the S3 INC position is required for normal channel function. The S3 INC is invariably an Asp, and we used conventional site-directed mutagenesis to introduce Asn in the S3 INC positions in all four domains (Asp197Asn, Asp646Asn, Asp1101Asn, and Asp1420Asn). Despite this less subtle perturbation of the native Asp side chains, we observed no statistically significant changes in the G-V in DI through DIV (Fig. 3 C and Table 1). In contrast, neutralizing the Asp side chains by Asn slowed the entry into fast inactivation in DII and DIV, and changed SSI values in DIII and DIV (Fig. 3 D and Table 1).

Leu substitutions in the S2 HC results in potent functional changes in DII–DIV

To explore the function of the extremely conserved aromatic side chain that constitutes the S2 HC, we turned to conventional site-directed mutagenesis and, domain by domain, replaced the native $Na_v1.4$ aromatic side chain by Leu (Fig. 4, A and B). Mutating Tyr168 in DI to Leu did not result in significant changes on the G-V relationship or the SSI (Fig. 4, C and D, and Table 1), suggesting that neither the aromatic character nor the hydroxyl moiety of the native Tyr side chain is of critical importance to channel function. In contrast, replacing the equivalent Phe side chain in DII to DIV resulted in significant changes in the G-V and the SSI: Phe621Leu (DII) and Phe1396Leu (DIV) significantly shifted both of these parameters to more hyperpolarized potentials, whereas the Phe1076Leu mutation (DIII) resulted in a significant change in the opposite direction (Fig. 4, C and D, and Table 1). The significant left-shift in the G-V of Phe1396Leu was accompanied by a slowing of the entry into fast inactivation (Fig. 4 D). Collectively, these data highlight a surprising asymmetry in the functional effects arising from equivalent mutations in the four domains.

The electrostatic surface potential (ESP) of the S2 HC does not play a role in channel function

Although the nonaromatic Leu substitution in the HC had little impact on channel function in DI, the changes observed in DII–DIV raised the possibility that the negative ESP of the Phe side chains could contribute to channel function. In particular, so-called cation–pi interactions have been found between the face of aromatic side chains and positively charged moieties such as ammonium compounds or basic side chains (Burley and Petsko, 1986;

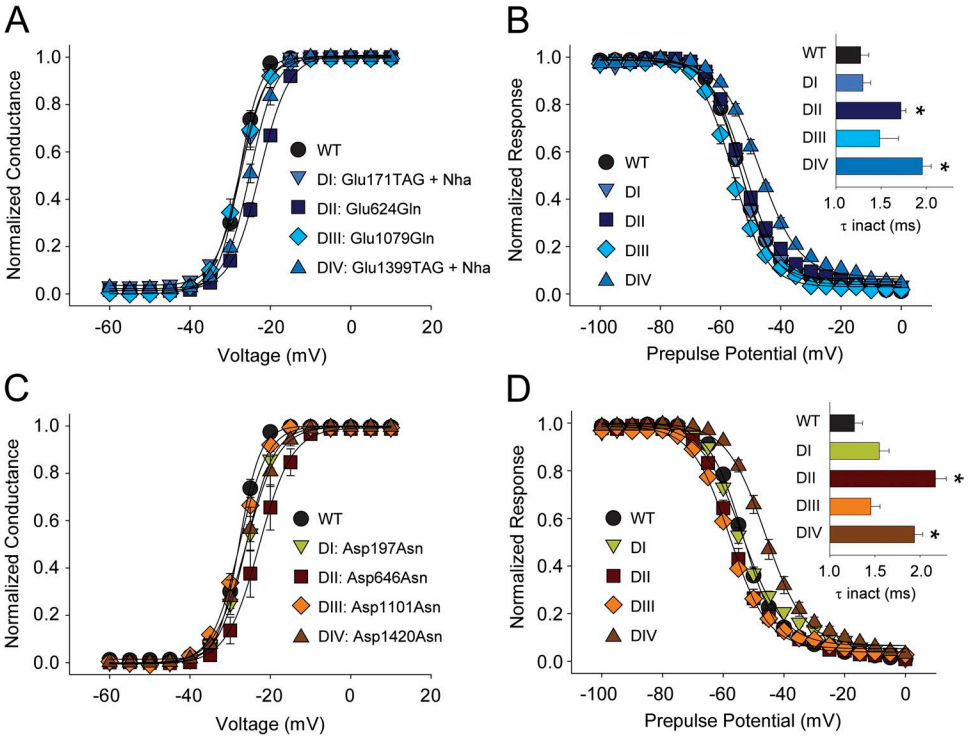

Figure 3. Removing the negative charge in the INC has little effect on channel activation. (A and B) G-V (A) and SSI curves (B) for WT and mutants in which the S2 INC was neutralized through introduction of Nha or Gln (DI, Glu171TAG + Nha; DII, Glu624Gln; DIII, Glu1079Gln; DIV, Glu1399TAG + Nha). (C and D) G-V (C) and SSI curves (D) for WT and mutants in which the S3 INC was neutralized through the introduction of Asn (DI, Asp197Asn; DII, Asp646Asn; DIII, Asp1101Asn; DIV, Asp1420Asn). The insets in B and D show bar graphs representing the average time constants for fast inactivation (τ) for a depolarizing voltage step to −15 mV. *, statistical difference to WT values in an unpaired *t* test ($P < 0.01$).

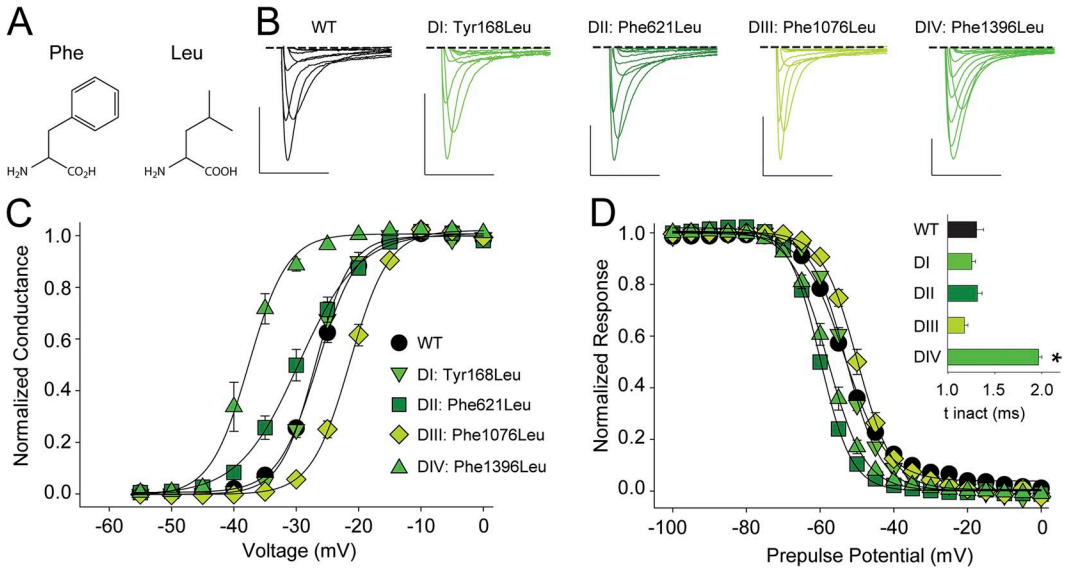

Figure 4. Replacing the S2 aromatic with Leu has drastic functional consequences in DII–DIV. (A) Chemical structure of Phe and Leu. (B) Sample traces for currents recorded from WT or mutants that replaced the S2 aromatic with Leu (DI, Tyr168Leu; DII, Phe621Leu; DIII, Phe1076Leu; DIV, Phe1396Leu). Bars: horizontal, 5 ms; vertical, 500 nA. Voltage steps were from −40 to +20 mV in 10-mV increments. (C and D) G-V (C) and SSI curves (D) for WT and mutants in which the S2 aromatic was replaced by Leu; the inset in D shows a bar graph representing the average time constants for fast inactivation (τ) for a depolarizing voltage step to −15 mV for WT and the Leu mutants in DI–DIV. *, statistical difference to WT values in an unpaired *t* test ($P < 0.01$).

Dougherty, 1996). Given that the conserved aromatic side chain in S2 is in close physical proximity to the S4 gating charges (Fig. 1), we reasoned that such an interaction could potentially explain the phenotypes observed with Phe621Leu, Phe1076Leu, and Phe1396Leu, as these mutations would abolish electrostatic interactions between the face of the aromatic side chain in S2 and positive charges in S4, a possibility suggested previously

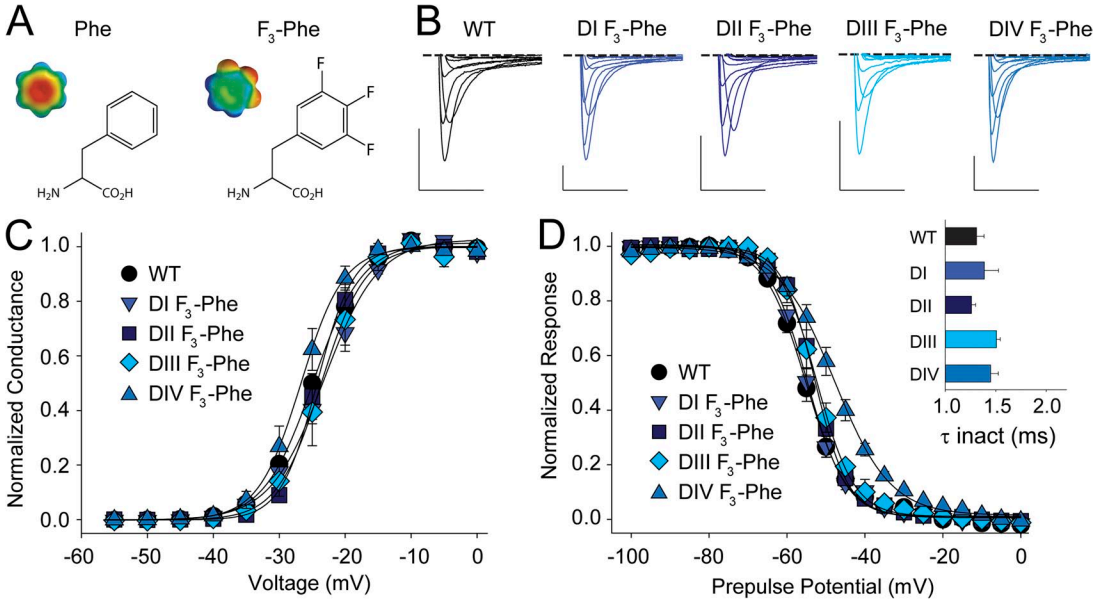

Figure 5. Removing the negative ESP of the S2 aromatic has minimal functional consequences. (A) Chemical structures and ESP maps of Phe and 3,4,5-trifluoro-Phe (F_3-Phe) (ESP: red, −25 kcal/mol; green, 0 kcal/mol; blue, +25 kcal/mol; see Pless et al., 2011a, for details). (B) Sample traces for currents recorded from WT or mutants in which F_3-Phe has been introduced in the S2 HC (DI, Tyr168TAG + F_3-Phe; DII, Phe621TAG + F_3-Phe; DIII, Phe1076TAG + F_3-Phe; DIV, Phe1396TAG + F_3-Phe). Bars: horizontal, 5 ms; vertical, 500 nA. Voltage steps were from −40 to +20 mV in 10-mV increments. (C and D) G-V (C) and SSI curves (D) for WT and mutants in which the S2 aromatic was replaced by F_3-Phe; the inset in D shows a bar graph representing the average time constants for fast inactivation (τ) for a depolarizing voltage step to −15 mV for WT and the F_3-Phe mutants in DI–DIV.

in early potassium channel structures (Long et al., 2005). We thus used fluorinated derivatives of Phe, an approach that has been extensively used to disperse the pi electron cloud of aromatic side chains to uncover cation–pi interactions in several contexts (Zhong et al., 1998; Santarelli et al., 2007; Pless et al., 2011a). Trifluorination of Phe (F_3-Phe; Fig. 5, A and B) abolishes any cation–pi-binding ability without significantly affecting other physico-chemical properties of the side chain, such as size, hydrophobicity, or H-bonding ability. Thus, we introduced this unnatural Phe derivative in the S2 HC of DI–DIV. Consistent with our finding that a nonaromatic substitution of position 168 in DI (Tyr168Leu; Fig. 4) did not result in significant changes in G-V or SSI, the incorporation of F_3-Phe in the same position (Phe168TAG + F_3-Phe) also did not change these functional parameters (Fig. 5, C and D, and Table 1). Similarly, we found that the introduction of F_3-Phe in DII–DIV (Phe621TAG + F_3-Phe, Phe1076TAG + F_3-Phe, and Phe1396TAG + F_3-Phe, respectively) resulted in no significant changes in the G-V (Fig. 5, C and D, and Table1) or entry into fast inactivation (Fig. 5 C). Further, the SSI was not affected in DII and DIII, but showed a modest but significant right-shift with fluorination in DIV. However, because the Leu substitution in this position resulted in a left-shift of the SSI (Phe1396Leu; Fig. 4), the observed right-shift with F_3-Phe is likely caused by an effect specific to fluorination rather than suggesting a cation–pi interaction.

Tryptophan (Trp) substitutions highlight distinct roles for S2 HC in different VSDs

Similar to Phe, Trp side chains are aromatic in nature but are larger and also capable of H-bonding via their indole nitrogen (Fig. 6 A). Interestingly, Trp side chains introduced at the position of the highly conserved aromatic in S2 can stabilize open or closed conformations in *Shaker* potassium channels, depending on the presence and position of a Lys side chain in S4 (Tao et al., 2010). Further, it has been shown that the open-state stabilization observed in *Shaker* is mediated by a cation–pi interaction between the introduced Trp and the native Lys at the cytoplasmatic end of S4, Lys374 (Pless et al., 2011b). If different VSDs were to show a high degree of structural and functional conservation, a similar phenotype would be expected in the VSDs of Na_v channels when a Trp is introduced into S2 HC. To test this possibility directly, we introduced Trp side chains individually in all four domains of $Na_v1.4$ (Tyr168Trp, Phe621Trp, Phe1076Trp, and Phe1396Trp). Despite Trp being substantially larger than the native Phe side chains (and also capable of H-bonding via the indole nitrogen), we observed no changes in the G-V relations in DII and DIV, whereas a Trp in DIII resulted in a small but significant right-shift (Fig. 6 C and Table 1). In contrast, a Trp in position 168 resulted in a drastic (15-mV) right-shift in the G-V and a significantly shallower slope factor (Fig. 6 C and Table 1). Importantly, none of the Trp

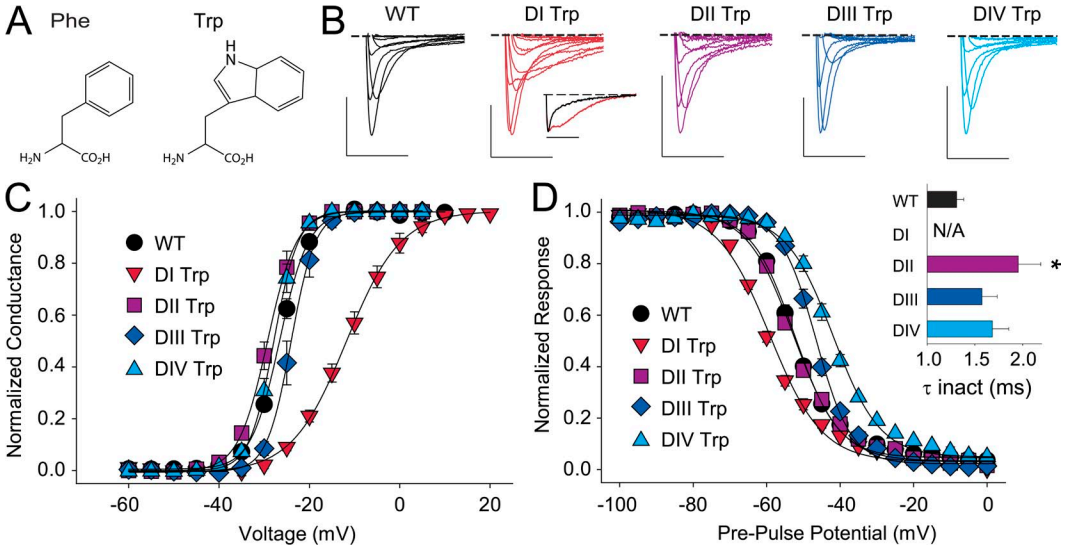

Figure 6. Introduction of a Trp highlights functional differences to potassium channel VSDs. (A) Chemical structure of Phe and Trp. (B) Sample traces for currents recorded from WT or mutants in which Trp has been introduced in the S2 HC (DI, Tyr168Trp; DII, Phe621Trp; DIII, Phe1076Trp; DIV, Phe1396Trp). The inset below DI Trp shows normalized currents recorded from WT (black) and the DI Trp mutant (red) in response to a depolarization to +15 mV. Bars: horizontal, 5 ms; vertical, 500 nA. Voltage steps were from −40 to +20 mV in 10-mV increments. (C and D) G-V (C) and SSI curves (D) for WT and mutants in which the S2 aromatic was replaced by Trp; the inset in D shows a bar graph representing the average time constants for fast inactivation (τ) for a depolarizing voltage step to −15 mV for WT and the Trp mutants in DI–DIV. *, statistical difference to WT values in an unpaired *t* test ($P < 0.01$). Note that the corresponding value for Tyr168Trp could not be determined because of the lack of significant ionic current at −15 mV.

substitutions mirrored the strong left-shift in the G-V observed in *Shaker* potassium channels. Interestingly, introducing Trp side chains in S2 changed the time course of inactivation in all four domains. Although Tyr168Trp in DI showed biphasic inactivation behavior at most voltages (see inset in Fig. 6 B), entry into fast inactivation was slower in DII–DIV, although this effect was statistically significant only in DII (Fig. 6 D). Furthermore, introducing Trp left-shifted the SSI in DI while resulting in a right-shifted SSI in DIII and DIV. In contrast, the Phe621Trp mutation modestly impacted the SSI or G-V relationships (Fig. 6 D and Table 1).

Finally, we sought to determine the molecular basis for the altered inactivation phenotype observed with Tyr168Trp in DI. Exchanging Trp for a Tyr not only reduces side chain volume but also introduces a very potent H-bond–donating group through the hydrogen on the Trp indole nitrogen. To test if the H-bonding ability of the introduced Trp side chain contributed to the observed phenotype, we incorporated a synthetic (and isosteric) Trp derivative, Ind (Fig. 7 A) (Lacroix et al., 2012) that lacks H-bonding ability. This substitution resulted in a mild left-shift in the G-V but abolished the biphasic inactivation behavior, and the SSI was reverted to values indistinguishable from WT (Fig. 7, B and C, and Table 2), strongly suggesting that the H-bonding ability of the introduced Trp indole nitrogen is the cause for the drastic inactivation phenotype of Tyr168Trp, possibly by trapping an intermediate inactivation state. In contrast, the effect on the channel G-V is likely to originate from either the steric perturbations or the larger pi electron cloud of Trp (compared with the native Tyr). However, we were unable to obtain significant currents with fluorinated Trp derivatives introduced in position 168 and could thus not distinguish between these possibilities.

DISCUSSION

VSDs confer voltage sensitivity to a variety of different membrane proteins (Bezanilla, 2008), and although some general properties can be transferred across different proteins (Lu et al., 2001; Bosmans et al., 2008; Arrigoni et al., 2013), it is not clear if the functional roles of conserved individual side chains is retained. This question is of particular relevance with regards to conserved acidic side chains in S1, S2, and S3 comprising ENC and INC, as well as the extremely conserved aromatic side chain in the S2 HC.

Charge plays a role for the voltage dependence of activation in the ENC but not the INC

Consistent with results obtained from both K_v and Na_v channels (Papazian et al., 1995; Seoh et al., 1996; Tiwari-Woodruff et al., 2000; DeCaen et al., 2008; Wu et al., 2010; Pless et al., 2011b; Yarov-Yarovoy et al., 2012), neutralization of the S2 ENC in DI results in a right-shift of the G-V. No charged side chain is present in the equivalent position of DII, but introduction of an acidic side chain here left-shifts the G-V (while introduction of a basic side chain right-shifts the G-V; Groome and Winston, 2013). This is in good agreement with previous results from a jellyfish K_v channel in which the introduction of a negatively charged side chain (which

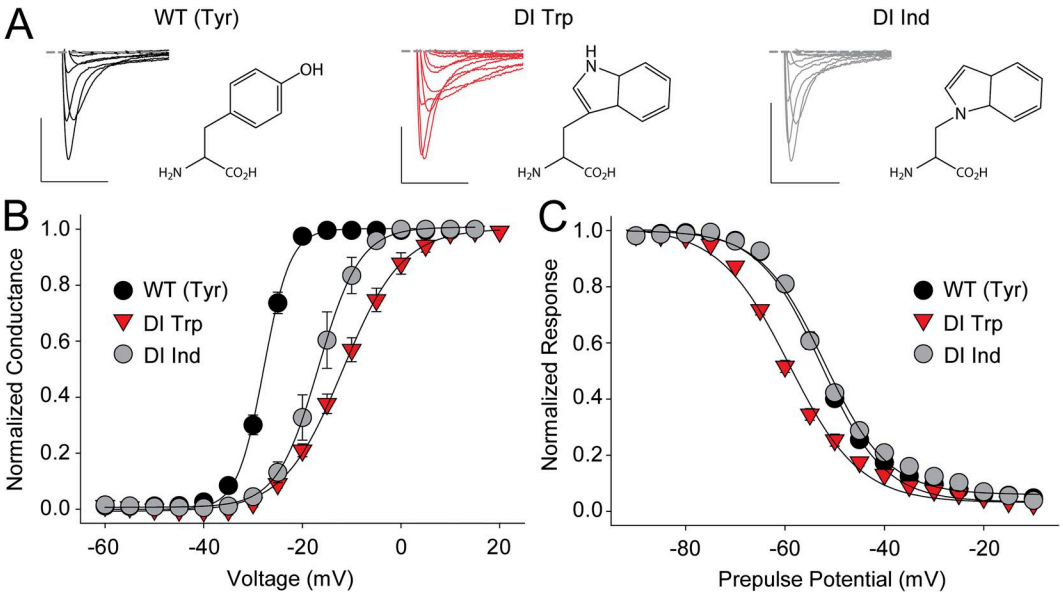

Figure 7. The disrupted inactivation phenotype of Tyr168Trp is caused by the Trp H-bonding ability. (A) Sample traces for currents recorded from WT and mutants that replaced the DI S2 Tyr with Trp or Ind, respectively (chemical structures are shown next to the current traces). Bars: horizontal, 5 ms; vertical, 500 nA. Voltage steps were from −40 to +20 mV in 10-mV increments. (B and C) G-V (B) and SSI curves (C) for WT and mutants in which the DI S2 Tyr was replaced with Trp or Ind.

is not present in the WT) stabilizes the channel open state (Klassen et al., 2008). These results contrast with the finding that neutralizations (or even charge reversals) in the S2 ENC of DIII and DIV have no effect on the voltage dependence of activation (Fig. 2 and Groome and Winston, 2013). Collectively, these results support the notion that charge plays a role in open-state stability in the S2 ENC in DI and DII, but not DIII and DIV.

Similar to our findings in the S2 ENC, we found that charge (or the absence of it) was only crucial for normal channel activation in S1 ENC of DI and DII, whereas neutralizations in DIII and DIV mostly affected channel inactivation, leaving channel activation largely unchanged. These domain-specific contributions are of particular interest in light of recent findings with a bacterial sodium channel that suggested a universal role of charge in the S1 ENC (Paldi and Gurevitz, 2010; DeCaen et al., 2011).

Importantly, the results from the S1 and the S2 ENC are qualitatively consistent: the DI S2 ENC is negatively charged and channel activation is right-shifted upon neutralization of this side chain, a result that is complemented by the fact the S1 ENC in DI is neutral, and the introduction of a negatively charged side chain leads to a left-shifted G-V. Our findings from the equivalent positions in DII were qualitatively identical: introducing a charge (S2 ENC) left-shifts the G-V, whereas removing a negatively charged side chain (S1 ENC) right-shifts the voltage dependence of activation. These results clearly argue for an important role of charge in the S1 and the S2 ENC of DI and DII, possibly by inherently (de)stabilizing the channel open conformation.

Interestingly, our results show that negative charge in the highly conserved INC positions is not a prerequisite for normal channel activation (Fig. 3) in DI, DIII, and DIV. We observed small right-shifts in the G-V relations when the DII S2 and S3 INC positions were neutralized. However, given that we were unable to introduce more subtle unnatural derivatives in the positions (624 and 646, respectively), we cannot distinguish if this indicates a critical contribution of (negative) charge or if the resulting phenotype is caused by the fact that the mutant channels contain a strong hydrogen bond donor group instead of a hydrogen bond acceptor group in a microenvironment evidently highly sensitive to substitutions (Cashin et al., 2007; Pless et al., 2011b,c).

Collectively, these data demonstrate a critical importance for charge only in the S2 ENC of DI and DII. In contrast, negative charge does not seem to play a major role for channel activation in the S2 ENC of DIII and DIV, nor the INC side chains in all four domains. Our results thus suggest that the latter positions do not contribute to energetically significant electrostatic interactions with S4 charges relevant for channel activation. Why, then, are these acidic side chains so highly conserved? An important clue comes from a naturally occurring mutation, which neutralizes the S3 INC side chain in the cardiac sodium channel isoform ($Na_v1.5$) and can result in cardiomyopathy and arrhythmia (Groenewegen et al., 2003; McNair et al., 2004): a recent study found that the mutation Asp1275Asn does not result in any major changes of the biophysical characteristics of the channel, but instead leads to a reduction in surface expression, leading to smaller but functionally unperturbed sodium currents (Watanabe et al., 2011). This raises the intriguing possibility that a major function of the negative charges in the INC (and to some extent ENC) is to assist protein folding and/or membrane insertion. In fact, this notion is supported by

TABLE 2

Electrophysiological effects of mutating the S2 HC

Construct	Location	G-V		SSI		*n*
		$V_{1/2}$	dx	$V_{1/2}$	dx	
WT	n/a	−26.3 ± 0.5	3.0 ± 0.1	−52.9 ± 0.5	5.7 ± 0.1	17
Tyr168Leu	DI S2 HC	−26.9 ± 0.6	2.7 ± 0.2	−52.8 ± 0.5	4.7 ± 0.1[a]	4
Phe621Leu	DII S2 HC	−29.7 ± 1.1[a]	4.4 ± 0.1[a]	−59.7 ± 0.4[a]	4.1 ± 0.1[a]	6
Phe1076Leu	DIII S2 HC	−21.6 ± 0.5[a]	2.8 ± 0.1	−50.3 ± 0.7[a]	4.6 ± 0.2[a]	8
Phe1396Leu	DIV S2 HC	−37.7 ± 1.3[a]	2.2 ± 0.3	−57.8 ± 0.9[a]	4.9 ± 0.2[a]	5
Tyr168TAG + F_3-Phe	DI S2 HC	−23.5 ± 0.9	3.8 ± 0.1	−54.6 ± 1.0	5.0 ± 0.4	4
Phe621TAG + F_3-Phe	DII S2 HC	−24.2 ± 0.9	2.6 ± 0.1	−52.6 ± 0.2	4.4 ± 0.1[a]	3
Phe1076TAG + F_3-Phe	DIII S2 HC	−23.5 ± 1.7	2.8 ± 0.2	−52.3 ± 1.2	4.8 ± 0.3[a]	4
Phe1396TAG + F_3-Phe	DIV S2 HC	−26.6 ± 1.1	2.9 ± 0.1	−47.6 ± 1.1[a]	7.3 ± 0.2[a]	6
Tyr168Trp	DI S2 HC	−11.6 ± 1.3[a]	5.8 ± 0.3[a]	−58.9 ± 0.6[a]	6.9 ± 0.3[a]	5
Phe621Trp	DII S2 HC	−29.1 ± 0.8	3.1 ± 0.2	−51.3 ± 1.4	6.4 ± 0.6	4
Phe1076Trp	DIII S2 HC	−23.7 ± 0.9[a]	2.2 ± 0.3	−46.5 ± 0.7[a]	4.6 ± 0.2[a]	8
Phe1396Trp	DIV S2 HC	−27.8 ± 0.5	2.7 ± 0.4	−39.1 ± 1.0[a]	6.5 ± 0.3[a]	4
Tyr168TAG + Ind	DI S2 HC	−16.5 ± 1.5[a]	3.8 ± 0.3	−51.4 ± 0.6	6.8 ± 0.3[a]	3

Displayed are the values for the midpoints ($V_{1/2}$) and the slope factors (dx) of the G-V relations and the SSI, as well as the number of experiments conducted (*n*).

[a]Statistical difference to WT values in an unpaired *t* test ($P < 0.01$).

extensive studies on K_v channels, where it has been demonstrated that the negative charges in S2 and S3 are critical for proper folding and membrane insertion of S4 gating charges, but not necessarily for channel function (Papazian et al., 1995; Tiwari-Woodruff et al., 1997; Sato et al., 2002, 2003; Zhang et al., 2007; Pless et al., 2011b; Cheng et al., 2013; Groome and Winston, 2013). Furthermore, given that countercharge neutralizations in most ENC and INC positions affect the voltage dependence of SSI (and/or entry into fast inactivation), these acidic side chains may play a role in shaping the precise fold of the intracellular protein surface (Pless et al., 2011b), a region strongly implicated in Na_v channel (fast) inactivation (McPhee et al., 1994, 1998; Ulbricht, 2005).

Defining the contributions of the S2 HC

Next, we set out to test if identical substitutions in the S2 HC caused similar effects in different domains of $Na_v1.4$. The results here clearly show that Leu substitutions can cause either hyperpolarizing (DII and DIV) or depolarizing shifts in the G-V (DIII), whereas no effect was observed in DI. Similarly, Trp substitutions shifted the G-V relations to more depolarizing voltages in DI and DIII only, whereas mutations in DII and DIV had no significant effect. These data not only highlight critical differences in the functional contributions of the S2 HC between different $Na_v1.4$ domains, but also point toward major differences compared with the VSDs of *Shaker* potassium channels: in the latter, Leu substitutions shift both the G-V and the Q-V to more depolarizing voltages, whereas Trp results in a hyperpolarizing shift of G-V and Q-V (Tao et al., 2010; Lacroix and Bezanilla, 2011), likely through the introduction of a cation–pi interaction between Trp290 and Lys374 (Pless et al., 2011b). Although a Lys is present in the equivalent position to *Shaker* Lys374 in both DI and DII of $Na_v1.4$ (Muroi et al., 2010; Payandeh et al., 2011) (in DIII and DIV they are occupied by Arg side chains), none of the domains showed the strong hyperpolarizing shift in the G-V observed with *Shaker* potassium channels.

Although structural studies in both Na_v and K_v channels have repeatedly shown the close physical proximity of the conserved aromatic side chain in the S2 HC to the gating charges of S4 (Payandeh et al., 2011, 2012; Zhang et al., 2012), our results clearly show that the S2 aromatic is not involved in an energetically significant cation–pi interaction, as the introduction of F_3-Phe in DI–DIV did not have significant effects on channel activation. This is also in good agreement with similar findings in *Shaker* potassium channels, where no such interaction could be identified for the native Phe side chain (Tao et al., 2010; Pless et al., 2011b). The absence of a cation–pi interaction, despite the close proximity of S2 aromatic and S4 charges, is most likely related to the strong orientation dependence of cation–pi interactions: unlike salt bridges, cation–pi interactions generally only occur if the cation assumes an ideal perpendicular orientation with regards to the face of the aromatic (Gallivan and Dougherty, 1999). The results therefore paint a differentiated picture of the functional contributions of the conserved S2 HC to channel activation in Na_v channels than expected from previous results with *Shaker* potassium channels: in DI, the main determinant appears to be side chain size, as only Trp resulted in a strong phenotype, but not the smaller Leu; in DII and DIV, the planarity (but not aromatic character) seems to be crucial because the introduction of the larger Trp caused no effect, whereas the nonplanar Leu resulted in functional changes; lastly, in DIII, both size and planarity are critical, as only Phe and F_3-Phe allow WT-like channel activation.

One potentially complicating factor with mutational studies on individual side chains in a large, pseudo-symmetric ion channel such as $Na_v1.4$ is the fact that they will affect only a single subunit, thus making it more difficult to detect more minute functional contributions. However, the results obtained by us (Table 2) and others (Muroi et al., 2010; Groome and Winston, 2013) clearly demonstrate that mutation of critical side chains for channel function results in clearly discernible phenotypes. We therefore believe that although phenotypes will be less pronounced than the equivalent mutations in the fourfold symmetric K_v channels, our approach still constitutes a valuable tool to decipher contributions of individual side chains within a large transmembrane protein such as $Na_v1.4$.

In conclusion, the results demonstrate that although some of the highly conserved VSD side chains (e.g., INC) show similar contributions in all four $Na_v1.4$ VSDs, as well as compared with K_v VSDs, for others (e.g., S2 HC), a high degree of amino acid conservation does not necessarily translate into a significant degree of functional conservation, neither among different domains of a given protein (i.e., DI–DIV in $Na_v1.4$) nor across different voltage-gated ion channels (i.e., VSDs from Na_v vs. K_v channels). In other words, even for highly conserved residues, the context often critically defines the functional contribution of a side chain. Thus, these results have implications for the functional extrapolation of conserved residues between channel types and likely functionally related protein families in general.

This work was supported by the Michael Smith Foundation for Health Research (to C.A. Ahern, H.T. Kurata, and S.A. Pless), the Heart and Stroke Foundation of Canada (to C.A. Ahern and H.T. Kurata), the Canadian Institutes of Health Research (grants MOP-56858 and MOP-97998), and a Banting postdoctoral fellowship by the Canadian Institutes of Health Research (to S.A. Pless). C.A. Ahern is a member of the Membrane Protein Structural Dynamics Consortium, which is funded by the National Institutes of Health (NIH)/National Institute of General Medical Sciences grant number GM087519, and is funded by the NIH R01GM106569.

The authors declare no competing financial interests.

Kenton J. Swartz served as editor.

Submitted: 23 May 2013
Accepted: 21 March 2014

REFERENCES

Arrigoni, C., I. Schroeder, G. Romani, J.L. Van Etten, G. Thiel, and A. Moroni. 2013. The voltage-sensing domain of a phosphatase gates the pore of a potassium channel. *J. Gen. Physiol.* 141:389–395. http://dx.doi.org/10.1085/jgp.201210940

Bezanilla, F. 2008. How membrane proteins sense voltage. *Nat. Rev. Mol. Cell Biol.* 9:323–332. http://dx.doi.org/10.1038/nrm2376

Bosmans, F., M.F. Martin-Eauclaire, and K.J. Swartz. 2008. Deconstructing voltage sensor function and pharmacology in sodium channels. *Nature.* 456:202–208. http://dx.doi.org/10.1038/nature07473

Burley, S.K., and G.A. Petsko. 1986. Amino-aromatic interactions in proteins. *FEBS Lett.* 203:139–143. http://dx.doi.org/10.1016/0014-5793(86)80730-X

Capes, D.L., M. Arcisio-Miranda, B.W. Jarecki, R.J. French, and B. Chanda. 2012. Gating transitions in the selectivity filter region of a sodium channel are coupled to the domain IV voltage sensor. *Proc. Natl. Acad. Sci. USA.* 109:2648–2653. http://dx.doi.org/10.1073/pnas.1115575109

Cashin, A.L., M.M. Torrice, K.A. McMenimen, H.A. Lester, and D.A. Dougherty. 2007. Chemical-scale studies on the role of a conserved aspartate in preorganizing the agonist binding site of the nicotinic acetylcholine receptor. *Biochemistry.* 46:630–639. http://dx.doi.org/10.1021/bi061638b

Catterall, W.A. 2010. Ion channel voltage sensors: Structure, function, and pathophysiology. *Neuron.* 67:915–928. http://dx.doi.org/10.1016/j.neuron.2010.08.021

Cha, A., P.C. Ruben, A.L. George Jr., E. Fujimoto, and F. Bezanilla. 1999. Voltage sensors in domains III and IV, but not I and II, are immobilized by Na^+ channel fast inactivation. *Neuron.* 22:73–87. http://dx.doi.org/10.1016/S0896-6273(00)80680-7

Chanda, B., and F. Bezanilla. 2002. Tracking voltage-dependent conformational changes in skeletal muscle sodium channel during activation. *J. Gen. Physiol.* 120:629–645. http://dx.doi.org/10.1085/jgp.20028679

Cheng, Y.M., C.M. Hull, C.M. Niven, J. Qi, C.R. Allard, and T.W. Claydon. 2013. Functional interactions of voltage sensor charges with an S2 hydrophobic plug in hERG channels. *J. Gen. Physiol.* 142:289–303. http://dx.doi.org/10.1085/jgp.201310992

DeCaen, P.G., V. Yarov-Yarovoy, Y. Zhao, T. Scheuer, and W.A. Catterall. 2008. Disulfide locking a sodium channel voltage sensor reveals ion pair formation during activation. *Proc. Natl. Acad. Sci. USA.* 105:15142–15147. http://dx.doi.org/10.1073/pnas.0806486105

DeCaen, P.G., V. Yarov-Yarovoy, E.M. Sharp, T. Scheuer, and W.A. Catterall. 2009. Sequential formation of ion pairs during activation of a sodium channel voltage sensor. *Proc. Natl. Acad. Sci. USA.* 106:22498–22503. http://dx.doi.org/10.1073/pnas.0912307106

DeCaen, P.G., V. Yarov-Yarovoy, T. Scheuer, and W.A. Catterall. 2011. Gating charge interactions with the S1 segment during activation of a Na^+ channel voltage sensor. *Proc. Natl. Acad. Sci. USA.* 108:18825–18830. http://dx.doi.org/10.1073/pnas.1116449108

Delemotte, L., M. Tarek, M.L. Klein, C. Amaral, and W. Treptow. 2011. Intermediate states of the Kv1.2 voltage sensor from atomistic molecular dynamics simulations. *Proc. Natl. Acad. Sci. USA.* 108:6109–6114. http://dx.doi.org/10.1073/pnas.1102724108

Dougherty, D.A. 1996. Cation-π interactions in chemistry and biology: A new view of benzene, Phe, Tyr, and Trp. *Science.* 271:163–168. http://dx.doi.org/10.1126/science.271.5246.163

Gallivan, J.P., and D.A. Dougherty. 1999. Cation-pi interactions in structural biology. *Proc. Natl. Acad. Sci. USA.* 96:9459–9464. http://dx.doi.org/10.1073/pnas.96.17.9459

Goldschen-Ohm, M.P., D.L. Capes, K.M. Oelstrom, and B. Chanda. 2013. Multiple pore conformations driven by asynchronous movements of voltage sensors in a eukaryotic sodium channel. *Nat Commun.* 4:1350. http://dx.doi.org/10.1038/ncomms2356

Groenewegen, W.A., M. Firouzi, C.R. Bezzina, S. Vliex, I.M. van Langen, L. Sandkuijl, J.P. Smits, M. Hulsbeek, M.B. Rook, H.J. Jongsma, and A.A. Wilde. 2003. A cardiac sodium channel mutation cosegregates with a rare connexin40 genotype in familial atrial standstill. *Circ. Res.* 92:14–22. http://dx.doi.org/10.1161/01.RES.0000050585.07097.D7

Groome, J.R., and V. Winston. 2013. S1–S3 counter charges in the voltage sensor module of a mammalian sodium channel regulate fast inactivation. *J. Gen. Physiol.* 141:601–618. http://dx.doi.org/10.1085/jgp.201210935

Hille, B. 2001. Ion Channels of Excitable Membranes. Third edition. Sinauer, Sunderland, MA. 814 pp.

Klassen, T.L., M.L. O'Mara, M. Redstone, A.N. Spencer, and W.J. Gallin. 2008. Non-linear intramolecular interactions and voltage sensitivity of a K_V1 family potassium channel from *Polyorchis penicillatus* (Eschscholtz 1829). *J. Exp. Biol.* 211:3442–3453. http://dx.doi.org/10.1242/jeb.022608

Lacroix, J.J., and F. Bezanilla. 2011. Control of a final gating charge transition by a hydrophobic residue in the S2 segment of a K^+ channel voltage sensor. *Proc. Natl. Acad. Sci. USA.* 108:6444–6449. http://dx.doi.org/10.1073/pnas.1103397108

Lacroix, J.J., S.A. Pless, L. Maragliano, F.V. Campos, J.D. Galpin, C.A. Ahern, B. Roux, and F. Bezanilla. 2012. Intermediate state trapping of a voltage sensor. *J. Gen. Physiol.* 140:635–652. http://dx.doi.org/10.1085/jgp.201210827

Lin, M.C., J.Y. Hsieh, A.F. Mock, and D.M. Papazian. 2011. R1 in the Shaker S4 occupies the gating charge transfer center in the resting state. *J. Gen. Physiol.* 138:155–163. http://dx.doi.org/10.1085/jgp.201110642

Long, S.B., E.B. Campbell, and R. Mackinnon. 2005. Crystal structure of a mammalian voltage-dependent Shaker family K^+ channel. *Science.* 309:897–903. http://dx.doi.org/10.1126/science.1116269

Lu, Z., A.M. Klem, and Y. Ramu. 2001. Ion conduction pore is conserved among potassium channels. *Nature.* 413:809–813. http://dx.doi.org/10.1038/35101535

McCusker, E.C., C. Bagnéris, C.E. Naylor, A.R. Cole, N. D'Avanzo, C.G. Nichols, and B.A. Wallace. 2012. Structure of a bacterial voltage-gated sodium channel pore reveals mechanisms of opening and closing. *Nat Commun.* 3:1102. http://dx.doi.org/10.1038/ncomms2077

McNair, W.P., L. Ku, M.R. Taylor, P.R. Fain, D. Dao, E. Wolfel, and L. Mestroni; Familial Cardiomyopathy Registry Research Group. 2004. SCN5A mutation associated with dilated cardiomyopathy, conduction disorder, and arrhythmia. *Circulation.* 110:2163–2167. http://dx.doi.org/10.1161/01.CIR.0000144458.58660.BB

McPhee, J.C., D.S. Ragsdale, T. Scheuer, and W.A. Catterall. 1994. A mutation in segment IVS6 disrupts fast inactivation of sodium channels. *Proc. Natl. Acad. Sci. USA.* 91:12346–12350. http://dx.doi.org/10.1073/pnas.91.25.12346

McPhee, J.C., D.S. Ragsdale, T. Scheuer, and W.A. Catterall. 1998. A critical role for the S4-S5 intracellular loop in domain IV of the sodium channel alpha-subunit in fast inactivation. *J. Biol. Chem.* 273:1121–1129. http://dx.doi.org/10.1074/jbc.273.2.1121

Muroi, Y., M. Arcisio-Miranda, S. Chowdhury, and B. Chanda. 2010. Molecular determinants of coupling between the domain III voltage sensor and pore of a sodium channel. *Nat. Struct. Mol. Biol.* 17:230–237. http://dx.doi.org/10.1038/nsmb.1749

Nowak, M.W., J.P. Gallivan, S.K. Silverman, C.G. Labarca, D.A. Dougherty, and H.A. Lester. 1998. In vivo incorporation of unnatural amino acids into ion channels in *Xenopus* oocyte expression

system. *Methods Enzymol.* 293:504–529. http://dx.doi.org/10.1016/S0076-6879(98)93031-2

Paldi, T., and M. Gurevitz. 2010. Coupling between residues on S4 and S1 defines the voltage-sensor resting conformation in NaChBac. *Biophys. J.* 99:456–463. http://dx.doi.org/10.1016/j.bpj.2010.04.053

Papazian, D.M., X.M. Shao, S.A. Seoh, A.F. Mock, Y. Huang, and D.H. Wainstock. 1995. Electrostatic interactions of S4 voltage sensor in Shaker K^+ channel. *Neuron.* 14:1293–1301. http://dx.doi.org/10.1016/0896-6273(95)90276-7

Payandeh, J., T. Scheuer, N. Zheng, and W.A. Catterall. 2011. The crystal structure of a voltage-gated sodium channel. *Nature.* 475:353–358. http://dx.doi.org/10.1038/nature10238

Payandeh, J., T.M. Gamal El-Din, T. Scheuer, N. Zheng, and W.A. Catterall. 2012. Crystal structure of a voltage-gated sodium channel in two potentially inactivated states. *Nature.* 486:135–139.

Planells-Cases, R., A.V. Ferrer-Montiel, C.D. Patten, and M. Montal. 1995. Mutation of conserved negatively charged residues in the S2 and S3 transmembrane segments of a mammalian K^+ channel selectively modulates channel gating. *Proc. Natl. Acad. Sci. USA.* 92:9422–9426. http://dx.doi.org/10.1073/pnas.92.20.9422

Pless, S.A., and C.A. Ahern. 2013. Unnatural amino acids as probes of ligand-receptor interactions and their conformational consequences. *Annu. Rev. Pharmacol. Toxicol.* 53:211–229. http://dx.doi.org/10.1146/annurev-pharmtox-011112-140343

Pless, S.A., J.D. Galpin, A. Frankel, and C.A. Ahern. 2011a. Molecular basis for class Ib anti-arrhythmic inhibition of cardiac sodium channels. *Nat Commun.* 2:351. http://dx.doi.org/10.1038/ncomms1351

Pless, S.A., J.D. Galpin, A.P. Niciforovic, and C.A. Ahern. 2011b. Contributions of counter-charge in a potassium channel voltage-sensor domain. *Nat. Chem. Biol.* 7:617–623. http://dx.doi.org/10.1038/nchembio.622

Pless, S.A., A.W. Leung, J.D. Galpin, and C.A. Ahern. 2011c. Contributions of conserved residues at the gating interface of glycine receptors. *J. Biol. Chem.* 286:35129–35136. http://dx.doi.org/10.1074/jbc.M111.269027

Santarelli, V.P., A.L. Eastwood, D.A. Dougherty, R. Horn, and C.A. Ahern. 2007. A cation-pi interaction discriminates among sodium channels that are either sensitive or resistant to tetrodotoxin block. *J. Biol. Chem.* 282:8044–8051. http://dx.doi.org/10.1074/jbc.M611334200

Sato, Y., M. Sakaguchi, S. Goshima, T. Nakamura, and N. Uozumi. 2002. Integration of Shaker-type K^+ channel, KAT1, into the endoplasmic reticulum membrane: Synergistic insertion of voltage-sensing segments, S3–S4, and independent insertion of pore-forming segments, S5–P–S6. *Proc. Natl. Acad. Sci. USA.* 99:60–65. http://dx.doi.org/10.1073/pnas.012399799

Sato, Y., M. Sakaguchi, S. Goshima, T. Nakamura, and N. Uozumi. 2003. Molecular dissection of the contribution of negatively and positively charged residues in S2, S3, and S4 to the final membrane topology of the voltage sensor in the K^+ channel, KAT1. *J. Biol. Chem.* 278:13227–13234. http://dx.doi.org/10.1074/jbc.M300431200

Schwaiger, C.S., P. Bjelkmar, B. Hess, and E. Lindahl. 2011. 3_{10}-helix conformation facilitates the transition of a voltage sensor S4 segment toward the down state. *Biophys. J.* 100:1446–1454. http://dx.doi.org/10.1016/j.bpj.2011.02.003

Schwaiger, C.S., S.I. Liin, F. Elinder, and E. Lindahl. 2013. The conserved phenylalanine in the K^+ channel voltage-sensor domain creates a barrier with unidirectional effects. *Biophys. J.* 104:75–84. http://dx.doi.org/10.1016/j.bpj.2012.11.3827

Seoh, S.A., D. Sigg, D.M. Papazian, and F. Bezanilla. 1996. Voltage-sensing residues in the S2 and S4 segments of the Shaker K^+ channel. *Neuron.* 16:1159–1167. http://dx.doi.org/10.1016/S0896-6273(00)80142-7

Sheets, M.F., J.W. Kyle, R.G. Kallen, and D.A. Hanck. 1999. The Na channel voltage sensor associated with inactivation is localized to the external charged residues of domain IV, S4. *Biophys. J.* 77:747–757. http://dx.doi.org/10.1016/S0006-3495(99)76929-8

Tao, X., A. Lee, W. Limapichat, D.A. Dougherty, and R. MacKinnon. 2010. A gating charge transfer center in voltage sensors. *Science.* 328:67–73. http://dx.doi.org/10.1126/science.1185954

Tiwari-Woodruff, S.K., C.T. Schulteis, A.F. Mock, and D.M. Papazian. 1997. Electrostatic interactions between transmembrane segments mediate folding of Shaker K^+ channel subunits. *Biophys. J.* 72:1489–1500. http://dx.doi.org/10.1016/S0006-3495(97)78797-6

Tiwari-Woodruff, S.K., M.A. Lin, C.T. Schulteis, and D.M. Papazian. 2000. Voltage-dependent structural interactions in the Shaker K^+ channel. *J. Gen. Physiol.* 115:123–138. http://dx.doi.org/10.1085/jgp.115.2.123

Ulbricht, W. 2005. Sodium channel inactivation: Molecular determinants and modulation. *Physiol. Rev.* 85:1271–1301. http://dx.doi.org/10.1152/physrev.00024.2004

Watanabe, H., T. Yang, D.M. Stroud, J.S. Lowe, L. Harris, T.C. Atack, D.W. Wang, S.B. Hipkens, B. Leake, L. Hall, et al. 2011. Striking in vivo phenotype of a disease-associated human *SCN5A* mutation producing minimal changes in vitro. *Circulation.* 124:1001–1011. http://dx.doi.org/10.1161/CIRCULATIONAHA.110.987248

West, J.W., D.E. Patton, T. Scheuer, Y. Wang, A.L. Goldin, and W.A. Catterall. 1992. A cluster of hydrophobic amino acid residues required for fast Na(+)-channel inactivation. *Proc. Natl. Acad. Sci. USA.* 89:10910–10914. http://dx.doi.org/10.1073/pnas.89.22.10910

Wu, D., K. Delaloye, M.A. Zaydman, A. Nekouzadeh, Y. Rudy, and J. Cui. 2010. State-dependent electrostatic interactions of S4 arginines with E1 in S2 during Kv7.1 activation. *J. Gen. Physiol.* 135:595–606. http://dx.doi.org/10.1085/jgp.201010408

Yang, N., and R. Horn. 1995. Evidence for voltage-dependent S4 movement in sodium channels. *Neuron.* 15:213–218. http://dx.doi.org/10.1016/0896-6273(95)90078-0

Yarov-Yarovoy, V., P.G. DeCaen, R.E. Westenbroek, C.Y. Pan, T. Scheuer, D. Baker, and W.A. Catterall. 2012. Structural basis for gating charge movement in the voltage sensor of a sodium channel. *Proc. Natl. Acad. Sci. USA.* 109:E93–E102. http://dx.doi.org/10.1073/pnas.1118434109

Zhang, L., Y. Sato, T. Hessa, G. von Heijne, J.K. Lee, I. Kodama, M. Sakaguchi, and N. Uozumi. 2007. Contribution of hydrophobic and electrostatic interactions to the membrane integration of the Shaker K^+ channel voltage sensor domain. *Proc. Natl. Acad. Sci. USA.* 104:8263–8268. http://dx.doi.org/10.1073/pnas.0611007104

Zhang, X., W. Ren, P. DeCaen, C. Yan, X. Tao, L. Tang, J. Wang, K. Hasegawa, T. Kumasaka, J. He, et al. 2012. Crystal structure of an orthologue of the NaChBac voltage-gated sodium channel. *Nature.* 486:130–134.

Zhong, W., J.P. Gallivan, Y. Zhang, L. Li, H.A. Lester, and D.A. Dougherty. 1998. From *ab initio* quantum mechanics to molecular neurobiology: A cation–π binding site in the nicotinic receptor. *Proc. Natl. Acad. Sci. USA.* 95:12088–12093. http://dx.doi.org/10.1073/pnas.95.21.12088